AGU PUBLICATIONS

Geophysical Research Letters

RESEARCH LETTER
10.1002/2017GL073217

Key Points:
- Daily to decadal variability of Asian-Australian summer monsoon rainfall increases in CMIP5 projections
- Fractional increases in variability are largest for the South Asian monsoon and smallest for the Australian monsoon
- Thermodynamic increases in atmospheric moisture can explain a large fraction of the increases in monsoon rainfall variability

Supporting Information:
- Supporting Information S1

Correspondence to:
J. R. Brown,
josephine.brown@bom.gov.au

Citation:
Brown, J. R., A. F. Moise, and R. A. Colman (2017), Projected increases in daily to decadal variability of Asian-Australian monsoon rainfall, *Geophys. Res. Lett.*, *44*, 5683–5690, doi:10.1002/2017GL073217.

Received 26 FEB 2017
Accepted 15 MAY 2017
Accepted article online 18 MAY 2017
Published online 3 JUN 2017

Projected increases in daily to decadal variability of Asian-Australian monsoon rainfall

Josephine R. Brown[1], Aurel F. Moise[1], and Robert A. Colman[1]

[1]Research and Development Division, Bureau of Meteorology, Melbourne, Australia

Abstract Changes in rainfall variability in future climate will pose challenges for adaptation. To evaluate changes in Asian-Australian monsoon wet season rainfall, daily data from historical and future (Representative Concentration Pathway "RCP8.5") climate simulations are band pass-filtered to isolate variability on near-daily, weekly, monthly, intraseasonal, annual, interannual, and decadal time scales. This method is used to quantify changes in variability from 35 coupled climate models for each time scale over the Australian, South Asian, and East Asian monsoon domains. In nearly all cases, the median model change is positive, indicating increased rainfall variability, although with large model spread. The role of increased atmospheric moisture is examined by estimating the change due to an idealized thermodynamic enhancement. This enhancement produces increases in variability that are within the range of the simulated changes under the RCP8.5 scenario, indicating that thermodynamic responses provide a first-order explanation for the increased daily to decadal monsoon rainfall variability.

1. Introduction

In a warmer climate, there is an expected increase in atmospheric water vapor concentration following the Clausius-Clapeyron relationship of about 6–7%/K, consistent with observations and model simulations of future climate, while global mean precipitation increases by only 2–3%/K due to radiative and evaporative constraints [*Held and Soden*, 2006; *Vecchi et al.*, 2006]. Increased atmospheric moisture content implies an overall enhancement of the climatological distribution of precipitation minus evaporation [*Durack et al.*, 2012], where regions with excess precipitation become wetter and those with greater evaporation become drier in the mean, although this mechanism does not apply over dry land areas [*Greve et al.*, 2014] or on regional scales where the spatial pattern of wet and dry regions may change [*Xie et al.*, 2010; *Chadwick et al.*, 2013]. On a regional scale, particularly in the tropics, spatial shifts in the position of wet or convective regions are the largest contribution to the pattern of rainfall change [*Chadwick et al.*, 2013; *Kent et al.*, 2015]. In a warmer world, there is expected to be an increase in the intensity of precipitation events, with a greater change for more intense events, leading to an increase in extreme precipitation [e.g., *Allan and Soden*, 2008; *Collins et al.*, 2013; *Hegerl et al.*, 2015]. Modes of climate variability such as El Niño–Southern Oscillation may also induce larger rainfall anomalies, regardless of whether the mode of variability is amplified [*Power et al.*, 2013; *Huang and Xie*, 2015].

Global monsoon projections based on Coupled Model Intercomparison Project Phase 5 (CMIP5) [*Taylor et al.*, 2012] models show an increase in total monsoon rainfall, largely due to increased atmospheric moisture content [*Christensen et al.*, 2013], despite slowing of tropical overturning circulations [*Held and Soden*, 2006; *Vecchi et al.*, 2006]. Analysis of regional monsoons for multiple Representative Concentration Pathways (RCPs) indicates increased seasonal mean rainfall for the Australian, South Asian, and East Asian monsoons [*Christensen et al.*, 2013]. However, there is a large intermodel spread in projected changes in mean summer monsoon rainfall, particularly for the Australian monsoon [*Brown et al.*, 2016]. Regional monsoons experience competing influences from thermodynamic and dynamic changes [e.g., *Endo and Kitoh*, 2014; *Brown et al.*, 2016].

Changes in the variability of monsoon rainfall may occur on a range of time scales. (Unless otherwise stated, rainfall "variability" is here defined as the standard deviation of rainfall.) For the global monsoon regions, such changes may have significant impacts when the intensity of rainfall events increases, for example, monsoon "burst" periods—periods of above average rainfall within the season [*Turner and Annamalai*, 2012; *Menon et al.*, 2013a]. As summarized by *Christensen et al.* [2013] in their Figure 14.4, both daily monsoon rainfall intensity and the variability of monsoon seasonal rainfall are expected to increase for the Australian-

Maritime Continent and East and South Asian summer monsoons under all emission scenarios considered, although model uncertainty is large for interannual changes, particularly for the Australian-Maritime Continent monsoon. The increases in several measures of monsoon rainfall variability suggest that variability on other time scales may also increase.

An increase in the interannual variability of global monsoon precipitation was found in a study of 19 CMIP5 models under the RCP4.5 scenario [*Hsu et al.*, 2013]. For the Indian (also known as South Asian) monsoon, *Menon et al.* [2013a] found that daily rainfall variability, measured as the standard deviation of daily rainfall, increased in future climate simulations under the RCP8.5 high emission scenario, with an average increase of 8 ± 4% per K warming. An increase in the interannual variability of Indian monsoon rainfall was also found [*Menon et al.*, 2013b]. By contrast, *Jourdain et al.* [2013] did not find a significant increase in the interannual variability of either Indian or Australian summer monsoon rainfall in the majority of their subset of skillful CMIP5 models. *Turner and Annamalai* [2012] considered a small sample of Coupled Model Intercomparison Project Phase 3 [*Meehl et al.*, 2007] models and found an increase in interannual variability of South Asian summer monsoon rainfall, with fewer normal years and more extreme wet or dry years.

None of these previous studies considered the consistency, or otherwise, changes in variability across a full range of time scales. In addition, they use a range of approaches in determining variability. In this study, variability of monsoon rainfall is calculated from daily data using band pass filtering to isolate variability on time scales from daily to decadal. We aim to summarize changes in monsoon rainfall variability across this wide range of time scales in an objective manner in order to determine whether there is a systematic increase in monsoon rainfall variability on multiple time scales and for different monsoon domains. We also address the question of whether there may be a common signal due to thermodynamic increases in atmospheric moisture content. To answer this simply, we calculate an idealized change due to thermodynamic processes and compare it with the magnitude of the simulated change.

2. Data and Methods

Daily precipitation and surface temperature data were obtained for 35 coupled models from the CMIP5 archive [*Taylor et al.*, 2012]. For a list of models used, see Table S1 in the supporting information. Simulations of historical climate (HIST, 1950–2000) and future climate under the high emission "RCP8.5" pathway (RCP8.5, 2050–2100) were used. The first realization ("run 1") was used for all models and simulations except for BCC-CSM1-1, for which "run 2" was used due to errors in the time coordinate for run 1. Model output was analyzed on the original model grid except where a multimodel mean was calculated (Figure 1) using data regridded to a common 1.5° grid. In addition, monthly mean surface temperature data were used to calculate mean temperature changes.

The model data are compared with precipitation observations from the Australian Water Availability Project (AWAP) high-quality data set [*Jones et al.*, 2009] for Australia and the Asian Precipitation Highly-Resolved Observational Data Integration Towards Evaluation (APHRODITE) [*Yatagai et al.*, 2012] for the South and East Asian monsoon domains. AWAP data are available on a 0.25° grid across the Australian continent from 1900 onward. APHRODITE contains continental-scale daily gridded precipitation at 0.25° resolution from 1951 onward based on a dense network of daily rain gauge data for Asia. In this study, AWAP data from 1950 to 2000 and APHRODITE data from 1951 to 2000 were used.

For each set of 50 years of model daily rainfall data, the climatological annual cycle was removed at each model grid point by subtracting the 50 year daily mean rainfall for each day. The area-weighted averages were then calculated over land areas within specified domains for each of the regional monsoons: Australia (AUS, 10°S–20°S, 120°E–150°E), South Asia (SAS, 5°N–35°N, 60°E–100°E), and East Asia (EAS, 5°N–35°N, 100°E–125°E). Model grid points were designated as land if the fractional land coverage was greater than 30% in the land-sea mask. The domains are shown in Figure 1 and are similar to those used in many previous studies [e.g., *Turner and Annamalai*, 2012; *Christensen et al.*, 2013].

The area-average daily anomalies for the three monsoon domains were then detrended and band pass-filtered using the following bands: "daily" (1–5 days), "weekly" (5–10 days), "monthly" (25–35 days), "intraseasonal" (30–80 days), "annual" (300–400 days), "interannual" (2–8 years), and "decadal" (9–20 years) to isolate

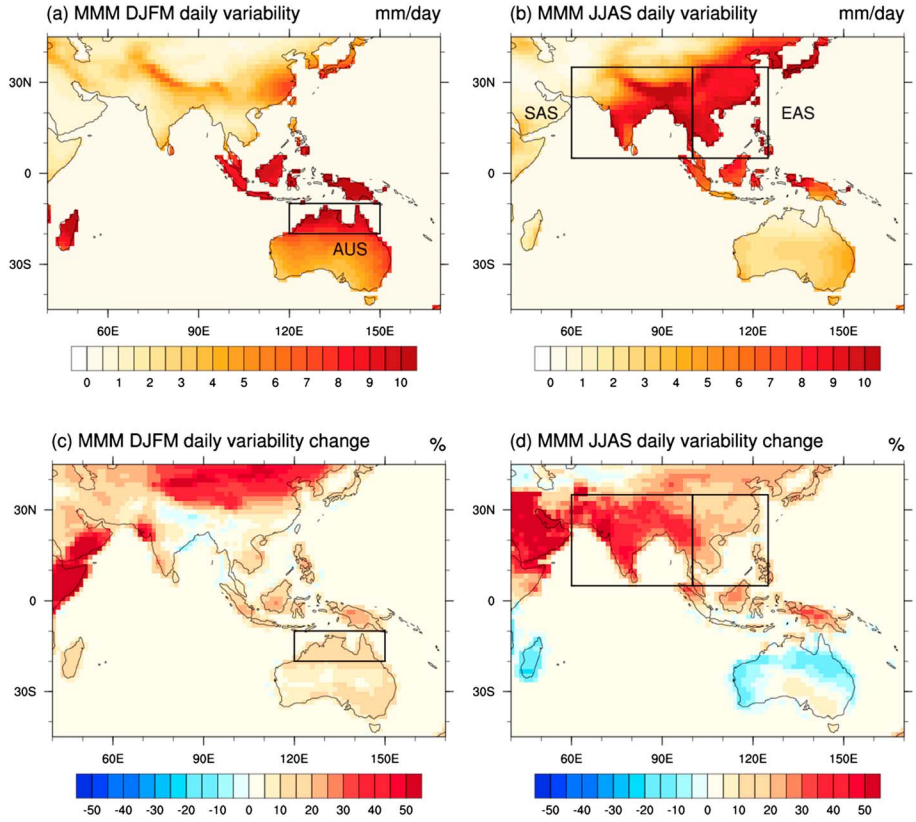

Figure 1. Multimodel mean standard deviation of daily rainfall anomalies (mm/d) over land in HIST (1950–2000) simulations for all days in (a) December to March and (b) June to September and change in standard deviation of daily rainfall anomalies (%) from HIST (1950–2000) to RCP8.5 (2050–2100) in (c) DJFM and (d) JJAS. The South Asian (SAS), East Asian (EAS), and Australian (AUS) monsoon domains are shown in the relevant wet season.

variability on these time scales. The band pass filtering accounted for the 360 day year in the Hadley Centre models. (Further discussion of the application of band pass filtering to the daily rainfall anomalies is provided in Figures S1 and S2 in the supporting information.) Finally, the filtered daily rainfall anomalies were extracted for monsoon wet season months only (December–March (DJFM) for Australia and June–September (JJAS) for South Asia and East Asia). The standard deviation of filtered daily area-average wet season rainfall anomalies was then calculated for each model for each band, and the difference between HIST and RCP8.5 rainfall standard deviations determined. While daily rainfall has a highly skewed distribution, particularly at station or grid point scale, this skewness is reduced when area average data are used and when daily anomalies from the long-term daily climatology are calculated (see Figure S3). The standard deviation is a descriptive statistic that can be used to describe the spread or variability of such rainfall anomalies, as in previous studies [e.g., *Menon et al.*, 2013a].

We note that the use of only 50 years of model output limits the robustness of calculated changes in decadal variability; however, this period was chosen to maximize the number of models with daily precipitation data for both scenarios. Analysis with a smaller set of models for a longer (95 year) period of HIST and RCP8.5 output produced similar results, including increases in decadal rainfall variability (not shown).

To quantify the influence of thermodynamic increases in atmospheric moisture content, an idealized enhancement due to the Clausius-Clapeyron ("CC") relationship was applied following the approach of *Allan and Soden* [2008], with the HIST average daily rainfall within the monsoon domain being multiplied by $7\% \times \Delta T$ where ΔT is the annual mean temperature change averaged over the same monsoon domain for RCP8.5 (2050–2100) minus HIST (1950–2000) for each model. This results in a fractional change in rainfall variability ($7\% \times \Delta T$) for each model for each domain, which is the same in each time band. This "CC" fractional change in rainfall variability can be compared with the fractional change from HIST to RCP8.5. The

relationship between increases in mean rainfall and increases in rainfall variability, implied by this idealized Clausius-Clapeyron enhancement, is examined further in sections 3 and 4.

3. Results

Before presenting the results from the band pass-filtered analysis, we examine the historical climatology and changes in unfiltered daily wet season rainfall variability in the models. The daily rainfall values are the anomalies from the 50 year daily climatology, as described in section 2. The multimodel mean daily variability for DJFM and JJAS in the HIST simulations (1950–2000) and the change in daily variability from HIST to RCP8.5 (2050–2100) are shown in Figure 1. The percentage change is calculated by first calculating the percentage change for individual models, then averaging those. The monsoon domains investigated in this study are also shown: Australia (AUS), South Asia (SAS), and East Asia (EAS).

As shown in Figures 1a and 1b, the Australian and Asian monsoon domains are regions of high daily rainfall variability in their respective wet seasons, although other tropical areas also experience high rainfall variability, as well as high daily rainfall amounts (see Figure S4). In the Southern Hemisphere wet season, DJFM (Figure 1c), the multimodel mean changes in daily wet season rainfall variability over northern Australia are positive, in the range 10–20%. Changes to the north over the Maritime Continent are also positive, indicating increased rainfall variability. In the Northern Hemisphere wet season, JJAS (Figure 1d), model-mean changes in rainfall variability over the South Asian and East Asian monsoon domains are also positive, with the largest changes (30–50%) seen in the South Asian monsoon domain. In summary, multimodel mean daily (wet season) rainfall variability increases in future climate for all three domains. This analysis is now extended to explore the full model spread and to determine whether similar increases occur on a range of time scales.

The variability of monsoon wet season rainfall for each of the monsoon domains was calculated using band pass-filtered daily anomalies for 50 years of the HIST and RCP8.5 simulations, following the method outlined in section 2 above. The spread of model rainfall variability, defined as the standard deviation of daily rainfall anomalies in each of the time bands listed in section 2, is shown in Figure 2 as a set of Tukey box plots. For each subplot in Figure 2, for each of the seven time bands, the spread of model variability in the HIST simulation is shown as the first (blue) box, while the spread in the RCP8.5 simulation is shown as the second (pink) box, and the difference RCP8.5 minus HIST is shown as the third set of (gray) boxes. Note that the values for the annual, interannual, and decadal time bands are multiplied by 5 in Figure 2 for clearer visualization. Also note that the results from the band pass-filtered analysis were compared with changes in variability from simple monthly mean, seasonal mean, and annual mean rainfall data, and similar results were obtained (not shown).

In Figure 2a, the variability for the Australian monsoon wet season (DJFM) months is shown. For all the domains, the use of area averages results in smoothing of small-scale variability associated with local convection and therefore may reduce the magnitude of near-daily variability relative to longer time scales. With this caveat, the largest variability is found in the intraseasonal band (30–80 days), consistent with the known influence of the Madden-Julian Oscillation on Australian monsoon rainfall [*Wheeler and McBride*, 2005; *Wheeler et al.*, 2009]. Variability is also large in the 5–10 day band, corresponding to the synoptic time scale of "burst and break" periods in the monsoon wet season [*Wheeler and McBride*, 2005]. As the 50 year average annual cycle is removed before filtering, the remaining variability in the "annual" time band represents deviation from this climatological annual cycle. The rainfall variability calculated from AWAP observations (shown as dark blue squares overlaid on the HIST box plots in Figure 2a) is generally within the model HIST interquartile range, indicating reasonable agreement between models and observations. The median change in variability is positive for all time bands (gray boxes), indicating that rainfall variability is increased in the majority of models. The lower quartile of models is above zero for daily, weekly, and intraseasonal bands, indicating strong model agreement on increased variability. However, there is large model spread, with negative values at the lower tail showing that for all time scales, some models simulate reduced future rainfall variability.

For the South Asian monsoon (Figure 2b), the largest variability in rainfall is also seen at weekly (5–10 days) and intraseasonal (30–80 days) time scales. The observed variability calculated over the South Asian monsoon domain using the APHRODITE data set for the period 1951–2000 is shown as dark blue squares in Figure 2b. There is generally good agreement between the model variability and observations, with the

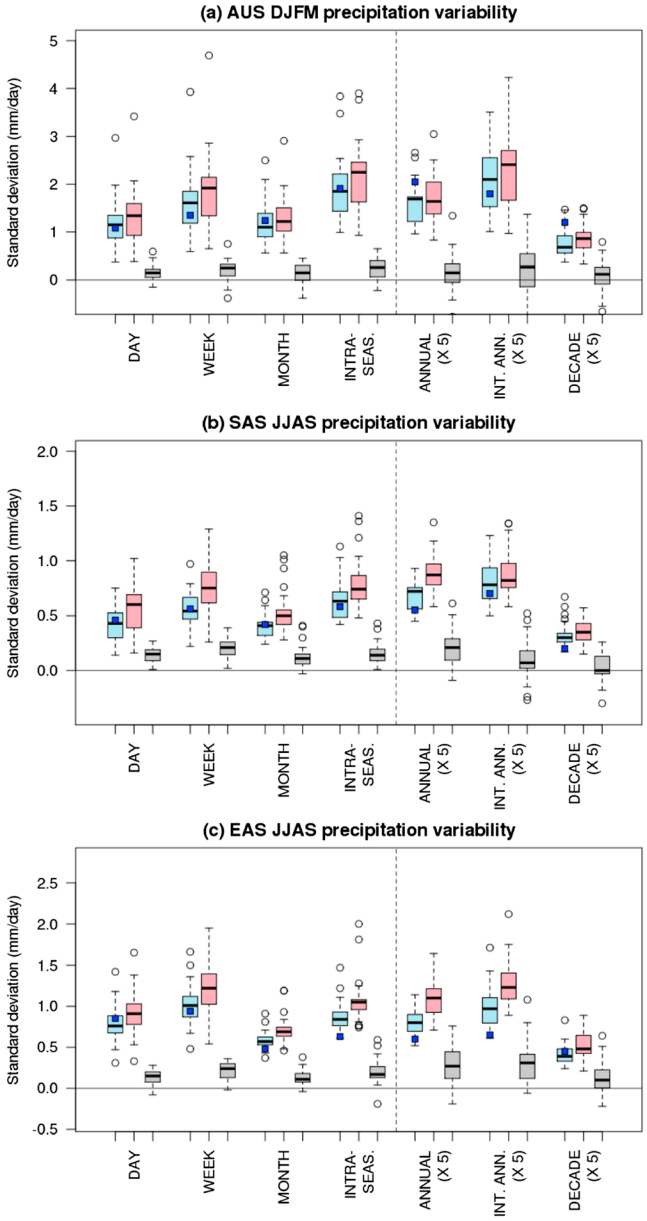

Figure 2. Standard deviation (mm/d) of summer monsoon rainfall for HIST (blue), RCP8.5 (pink), and difference (gray) for (a) AUS, (b) SAS, and (c) EAS domains (values are ×5 for annual, interannual, and decadal bands). Observations from (a) AWAP and (b and c) APHRODITE data sets are shown as dark blue squares. Note different *y* axes. The boxes show median and upper and lower quartiles, the whiskers indicate values within 1.5 interquartile ranges of the lower and upper quartiles, and the circles indicate outliers beyond this range.

observations lying within the interquartile range for all except decadal time scales. The difference between HIST and RCP8.5 model rainfall variability is generally positive for the SAS monsoon. For all time scales except decadal, the model difference (gray boxes) interquartile range lies clearly above zero, indicating that at least three quarters of models simulate increased rainfall variability in the warmer climate. For daily, weekly, and intraseasonal time scales, all models simulate an increase.

In the case of the East Asian monsoon (Figure 2c), HIST wet season (JJAS) rainfall variability is largest on "weekly" time scales (5–10 day band). There is generally good agreement with the observed EAS monsoon rainfall variability calculated from APHRODITE data. The observations lie within the model range, although at the lower end of the range for several time bands, indicating the model rainfall variability may be somewhat overestimated. The change in EAS summer monsoon rainfall variability is positive for at least three quarters of models for all time scales, although some models simulate reduced variability on each time scale.

The percentage change in rainfall variability for each of the monsoon domains is shown in Figure 3a to allow direct comparison, in particular allowing for the smaller absolute variability at longer time scales, and differences in absolute rainfall between regions. Figure 3a shows a median model increase in rainfall variability, generally between 10% and 40%, for all time scales. There is also a striking level of consistency across time scales for a given region. The larger variability increase in SAS compared with the other regions is found for daily to annual time scales. Model spread (for percentage changes) is greatest for the annual, interannual, and decadal bands, where changes are generally not greater than the interquartile range. Model agreement for increased rainfall variability is highest for the South and East Asian monsoons and lowest for the Australian monsoon, consistent with *Christensen et al.* [2013]. The larger uncertainty of changes in Australian monsoon rainfall variability may be linked to the large model spread in mean Australian monsoon rainfall changes, which is associated with biases in equatorial Pacific SSTs [*Brown et al.*, 2016].

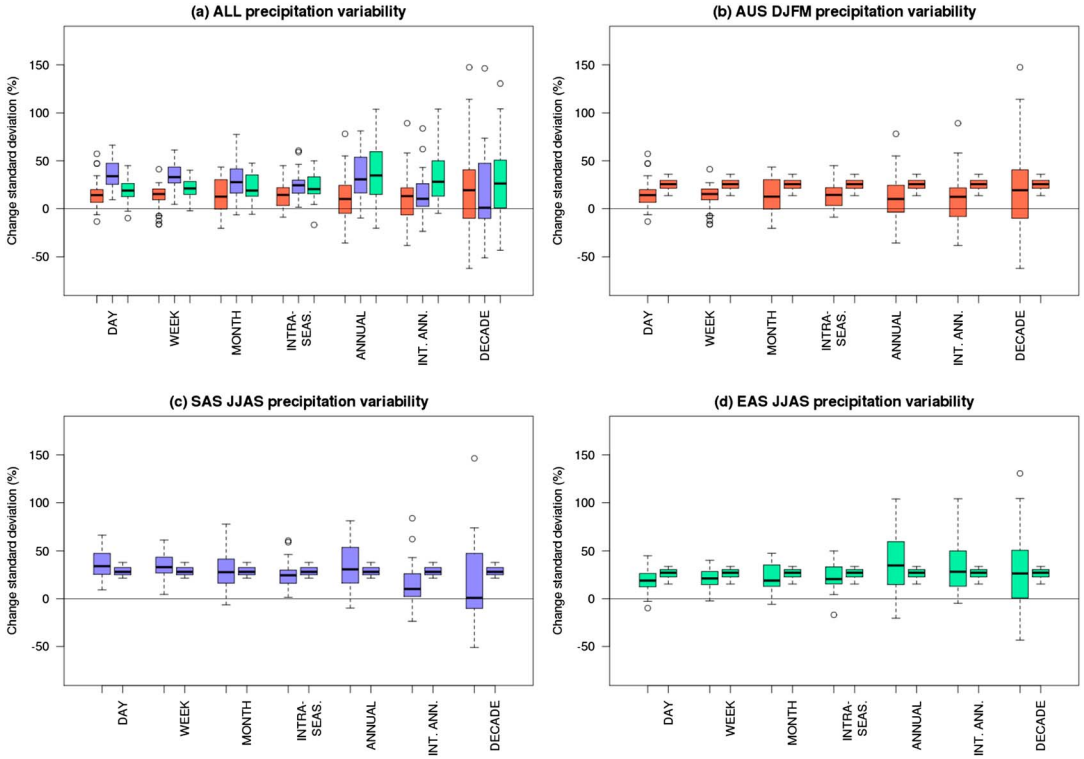

Figure 3. (a) RCP8.5 (2050–2100) minus HIST (1950–2000) differences in band pass-filtered daily rainfall standard deviation (%) for AUS (red, left boxes), SAS (purple, center boxes), and EAS (green, right boxes) monsoons and change in standard deviation (%) of summer monsoon rainfall for RCP8.5 minus HIST (left boxes) and idealized thermodynamic enhanced CC (right boxes) for (b) AUS, (c) SAS, and (d) EAS domains. Data are DJFM months for AUS and JJAS months for SAS and EAS.

A "null hypothesis" of direct relevance here is that increased monsoon rainfall variability may be a result of the higher atmospheric moisture content in a warmer climate, following the Clausius-Clapeyron relationship [e.g., *Held and Soden*, 2006; *Vecchi et al.*, 2006]. We therefore calculate an idealized enhancement of the daily monsoon rainfall, as outlined in section 2. The difference between the "CC" change in rainfall variability and the RCP8.5 change in rainfall variability, both compared with the unperturbed HIST climate, indicates how much of the simulated change under RCP8.5 may be due to this thermodynamic increase in atmospheric moisture.

For the Australian monsoon (Figure 3b), the median of the CC percentage change in rainfall variability is consistently larger than the median RCP8.5 change in variability for each time scale. However, there is a subset of models that simulates larger changes in variability than expected from the idealized thermodynamic response, implying positive contributions from dynamical changes. For the South Asian monsoon (Figure 3c), the median-simulated RCP8.5 changes are close to or slightly larger than the CC changes for daily, weekly, and annual time scales, and the thermodynamic null hypothesis provides a good estimate of the median model response over these time scales. However, RCP8.5 changes are much smaller than CC for interannual and decadal time scales, indicating that different combinations of processes are driving rainfall variability on the shorter and longer range of time scales considered. Where many models simulate RCP8.5 changes larger than the range of idealized thermodynamic change, this implies that dynamic changes in the monsoon circulation or other processes are contributing an additional strengthening influence on rainfall variability [e.g., *Christensen et al.*, 2013; *Chadwick et al.*, 2013; *Kent et al.*, 2015; *Brown et al.*, 2016].

In the case of the East Asian monsoon (Figure 3d), models simulate weaker changes in rainfall variability in RCP8.5 than CC for daily to intraseasonal time scales but, in contrast to SAS, show very similar or slightly larger changes in RCP8.5 than CC for annual to decadal time scales. Although uncertainties on these time scales are large due to sampling, it suggests that different mechanisms are operating in these two regions at these time scales, which warrant further investigation. As for the South Asian monsoon, this suggests a different

combination of processes driving rainfall variability change on subannual compared with annual to decadal time scales.

4. Discussion and Conclusions

The change in variability of Asian-Australian summer monsoon rainfall from historical (HIST) to future climate (RCP8.5) was investigated for a range of time scales from daily to decadal. Band pass filtering was used to isolate variability on each time scale, and the range of model rainfall standard deviations was calculated for HIST and RCP8.5 climates. Overall, a large majority of models simulated increased rainfall variability at all time scales and for all domains (with the exception of the South Asian monsoon at decadal time scales, where the median change was near zero). These results are consistent with previous studies finding increased Asian-Australian monsoon rainfall variability at subseasonal [*Christensen et al.*, 2013; *Menon et al.*, 2013a] and interannual [*Turner and Annamalai*, 2012; *Christensen et al.*, 2013; *Menon et al.*, 2013b] time scales. The absence of significant change identified by *Jourdain et al.* [2013] appears to be due to their smaller sample of models and more stringent criteria for significant changes in rainfall variability.

While the HIST monsoon rainfall variability is largest for the Australian summer monsoon, the fractional changes in RCP8.5 for this monsoon are generally smaller than for the South Asian or East Asian monsoons. The largest fractional increases in monsoon rainfall variability occur for the South Asian monsoon at all subannual time scales and for the East Asian monsoon at annual to decadal time scales. In addition, the models with the largest increase in variability are not the same across domains or across time scales, indicating that the signal is not dominated by a few particularly sensitive models.

The change in rainfall variability is not significantly correlated with the strength of historical simulation (HIST) variability except on annual, interannual, and decadal time scales (see Figures S5, S6, and S7), where correlations are negative and significant at the 5% level, indicating that models with smaller HIST variability simulate larger changes in variability. The lack of significant positive correlations at any time scale implies that the model spread in rainfall variability change is not due to the model spread in HIST rainfall variability.

Changes in rainfall variability are significantly positively correlated with changes in mean wet season rainfall for each of the monsoon domains for most time scales (see Figures S8, S9, and S10). In the case of the Australian monsoon (Figure S8), the change in mean rainfall explains up to 40% of the model spread in changes in monsoon rainfall variability (when both are expressed as percentage changes). Thus, models with negative changes in mean rainfall have negative or small positive changes in rainfall variability—and these models were found in a previous study to be less reliable due to larger equatorial Pacific SST biases [*Brown et al.*, 2016]. Significant positive correlations of similar magnitude were found between mean rainfall changes and rainfall variability changes for the South Asian and East Asian monsoons (Figures S9 and S10). While there is generally a strong relationship between increases in mean rainfall and rainfall variability, the relationship does not entirely explain the spread in model rainfall variability changes. In some cases, models simulate reduced mean rainfall but increased variability or the reverse (Figures S8, S9, and S10), and the variance explained from the relationship does not exceed 40% (maximum correlation coefficient $r = 0.64$ in Figure S8). Similarly, the large-scale spatial patterns of change in rainfall variability (Figure 1) have some agreement with spatial patterns of mean rainfall change (Figure S4), particularly in the sign of the changes. However, details of the spatial patterns of rainfall variability change are not explained by the mean rainfall changes.

The common increase across monsoon domains and time scales implies a role for common mechanisms. The most obvious is enhanced atmospheric moisture content, resulting in a thermodynamic increase in mean rainfall and also possibly the amplitude of rainfall variability. A comparison with the change due to an idealized rainfall anomaly increase by 7% per degree of warming indicates that the projected changes under the RCP8.5 emission scenario overlap with the range of this idealized Clausius-Clapeyron case for the South Asian and East Asian monsoon, but the Australian monsoon-projected change is generally smaller, suggesting the influence of dynamical changes weakening the monsoon variability [*Moise et al.*, 2012]. Alternatively, the thermodynamic response in this region may be smaller than the idealized enhancement of 7%/K and closer to the expected global average precipitation increase of 2–3%/K [e.g., *Held and Soden*, 2006]. A more detailed decomposition of changes in Australian monsoon rainfall variability is planned in a future study.

We note that the present study represents a highly simplified summary of changes over the three monsoon domains and does not attempt to uncover the specific processes driving rainfall variability changes on each time scale or for each domain. Instead, we highlight the common large-scale response of increased variability of Asian-Australian summer monsoon rainfall from daily to decadal time scales, which may have major social, economic, and environmental impacts. Further work is required to investigate the local and regional drivers of these changes and to reduce the remaining uncertainty in model projections.

Acknowledgments
The research presented in this paper was jointly supported by the Australian Bureau of Meteorology and the Australian Government's National Environmental Science Programme. We thank Andrew Dowdy and Simon Grainger for their comments on the manuscript. We acknowledge the World Climate Research Program's Working Group on Coupled Modeling, which is responsible for CMIP, and we thank the climate modeling groups (listed in Table S1 of this paper) for producing and making available their model output. For CMIP the U.S. Department of Energy's Program for Climate Model Diagnosis and Intercomparison provided coordinating support and led development of software infrastructure in partnership with the Global Organization for Earth System Science Portals. All CMIP5 model output used in this study can be obtained from the online database as listed at the PCMDI website: http://cmip-pcmdi.llnl.gov/cmip5/availability.html. For further information regarding model and observational data, analysis methods, and scripts, contact the first author.

References

Allan, R. P., and B. J. Soden (2008), Atmospheric warming and the amplification of precipitation extremes, *Science*, *321*, 1481–1484.

Chadwick, R., I. Boutle, and G. Martin (2013), Spatial patterns of precipitation change in CMIP5: Why the rich do not get richer in the tropics, *J. Clim.*, *26*, 3803–3822, doi:10.1175/JCLI-D-12-00543.1.

Christensen, J. H., et al. (2013), Climate phenomena and their relevance for future regional climate change, in *Climate Change 2013: The Physical Science Basis*, edited by T. F. Stocker et al., pp. 1217–1308, Cambridge Univ. Press, Cambridge, U. K., and New York.

Collins, M., et al. (2013), Long term climate change: Projections, commitments and irreversibility, in *Climate Change 2013: The Physical Science Basis*, edited by T. F. Stocker et al., pp. 1029–1136, Cambridge Univ. Press, Cambridge.

Durack, P., S. E. Wijffels, and R. J. Matear (2012), Ocean salinities reveal strong global water cycle intensification during 1950 to 2000, *Science*, *336*, 455–458, doi:10.1126/science.1212222.

Endo, H., and A. Kitoh (2014), Thermodynamic and dynamic effects on regional monsoon rainfall changes in a warmer climate, *Geophys. Res. Lett.*, *41*, 1704–1710, doi:10.1002/2013GL059158.

Greve, P., B. Orlowsky, B. Mueller, J. Sheffield, M. Reichstein, and S. I. Seneviratne (2014), Global assessment of trends in wetting and drying over land, *Nat. Geosci.*, *7*(10), 716–721, doi:10.1038/ngeo2247.

Hegerl, G., et al. (2015), Challenges in quantifying changes in the global water cycle, *Bull. Am. Meteorol. Soc.*, *96*, 1097–1115, doi:10.1175/BAMS-D-13-00212.1.

Held, I. M., and B. J. Soden (2006), Robust responses of the hydrological cycle to global warming, *J. Clim.*, *19*, 5686–5699, doi:10.1175/JCLI3990.1.

Hsu, P.-C., T. Li, H. Murakami, and A. Kitoh (2013), Future change of the global monsoon revealed from 19 CMIP5 models, *J. Geophys. Res. Atmos.*, *118*, 1247–1260, doi:10.1002/jgrd.50145.

Huang, P., and S. P. Xie (2015), Mechanisms of change in ENSO-induced tropical Pacific rainfall variability in a warming climate, *Nat. Geosci.*, *8*, 922–926, doi:10.1038/ngeo2571.

Jones, D. A., W. Wang, and R. Fawcett (2009), High-quality spatial climate data-sets for Australia, *Aust. Meteorol. Oceanogr. J.*, *58*, 233–248.

Jourdain, N. C., A. Sen Gupta, A. S. Taschetto, C. C. Ummenhofer, A. F. Moise, and K. Ashok (2013), The Indo-Australian monsoon and its relationship to ENSO and IOD in reanalysis data and the CMIP3/CMIP5 simulations, *Clim. Dyn.*, *41*, 3073–3102, doi:10.1007/s00382-013-1676-1.

Kent, C., R. Chadwick, and D. P. Rowell (2015), Understanding uncertainties in future projections of seasonal tropical precipitation, *J. Clim.*, *28*, 4390–4413, doi:10.1175/JCLI-D-14-00613.1.

Meehl, G. A., C. Covey, T. Delworth, M. Latif, B. McAvaney, J. F. B. Mitchell, R. J. Stouffer, and K. E. Taylor (2007), The WCRP CMIP3 multi-model dataset: A new era in climate change research, *Bull. Am. Meteorol. Soc.*, *88*, 1383–1394.

Menon, A., A. Levermann, and J. Schewe (2013a), Enhance future variability during India's rainy season, *Geophys. Res. Lett.*, *40*, 3242–3247, doi:10.1002/grl.50583.

Menon, A., A. Levermann, J. Schewe, J. Lehmann, and K. Frieler (2013b), Consistent increase in Indian monsoon rainfall and its variability across CMIP-5 models, *Earth Syst. Dyn.*, *4*, 987–300, doi:10.5194/esd-4-287-2013.

Moise, A. F., R. A. Colman, and J. R. Brown (2012), Behind uncertainties in projections of Australian tropical climate: Analysis of 19 CMIP3 models, *J. Geophys. Res.*, *117*, D10103, doi:10.1029/2011JD017365.

Brown, J. R., A. F. Moise, R. Colman, and H. Zhang (2016), Will a warmer world mean a wetter or drier Australian monsoon?, *J. Clim.*, *29*, 4577–4596, doi:10.1175/JCLI-D-15-0695.1.

Power, S., F. Delage, C. Chung, G. Kociuba, and K. Keay (2013), Robust twenty-first-century projections of El Niño and related precipitation variability, *Nature*, *502*, 541–545, doi:10.1038/nature12580.

Taylor, K. E., R. J. Stouffer, and G. A. Meehl (2012), An overview of CMIP5 and the experiment design, *Bull. Am. Meteorol. Soc.*, *93*, 485–498, doi:10.1175/BAMS-D-11-00094.1.

Turner, A. G., and H. Annamalai (2012), Climate change and the South Asian summer monsoon, *Nat. Clim. Change*, *2*, 587–595, doi:10.1038/NCLIMATE1495.

Vecchi, G. A., B. J. Soden, A. T. Wittenberg, I. M. Held, A. Leetmaa, and M. J. Harrison (2006), Weakening of tropical Pacific atmospheric circulation due to anthropogenic forcing, *Nature*, *441*, 73–76, doi:10.1038/nature04744.

Wheeler, M. C., and J. L. McBride (2005), Australian–Indonesian monsoon, in *Intraseasonal Variability in the Atmosphere-Ocean Climate System*, edited by W. K. M. Lau and D. E. Waliser, pp. 125–173, Springer, Berlin.

Wheeler, M. C., H. H. Hendon, S. Cleland, H. Meinke, and A. Donald (2009), Impacts of the Madden-Julian Oscillation on Australian rainfall and circulation, *J. Clim.*, *22*(6), 1482–1498, doi:10.1175/2008JCLI2595.1.

Xie, S.-P., C. Deser, G. A. Vecchi, J. Ma, H. Teng, and A. T. Wittenberg (2010), Global warming pattern formation: Sea surface temperature and rainfall, *J. Clim.*, *23*, 966–986, doi:10.1175/2009JCLI3329.1.

Yatagai, A., K. Kamiguchi, O. Arakawa, A. Hamada, N. Yasutomi, and A. Kitoh (2012), APHRODITE: Constructing a long-term daily gridded precipitation dataset for Asia based on a dense network of rain gauges, *Bull. Am. Meteorol. Soc.*, *93*, 1401–1415, doi:10.1175/BAMS-D-11-00122.1.